Journal of Magnetic Resonance **148,** 31–34 (2001)
doi:10.1006/jmre.2000.2219, available online at http://www.idealibrary.com on IDEAL®

Molecular Oxygen Spin–Lattice Relaxation in Solutions Measured by Proton Magnetic Relaxation Dispersion

Ching-Ling Teng, Heedoek Hong, Suzanne Kiihne, and Robert G. Bryant

Chemistry Department and Interdisciplinary Program in Biophysics, University of Virginia, Charlottesville, Virginia 22901-4319

Received April 4, 2000; revised July 31, 2000

Proton spin–lattice relaxation rate constants have been measured as a function of magnetic field strength for water, water–glycerol solution, cyclohexane, methanol, benzene, acetone, acetonitrile, and dimethyl sulfoxide. The magnetic relaxation dispersion is well approximated by a Lorentzian shape. The origin of the relaxation dispersion is identified with the paramagnetic contribution from molecular oxygen. In the small molecule cases studied here, the effective correlation time for the electron-nuclear coupling may include contributions from both translational diffusion and the electron T_1. The electron T_1 for molecular oxygen dissolved in several solvents was found to be approximately 7.5 ps and nearly independent of solvent or viscosity.

Key Words: **oxygen; magnetic relaxation; relaxation dispersion; MRD; electron-spin relaxation.**

Recent applications of molecular oxygen as a relaxation agent to define how oxygen interacts with macromolecules like a folded protein give new importance to understanding the electron-spin relaxation in molecular oxygen (*1*). Molecular oxygen is well known to alter the magnetic relaxation rates of nuclear and electron spin resonances; however, the electron spin relaxation properties of oxygen itself are not well characterized (*2–5*). The EPR spectrum is usually inaccessible because the lines are broad; however, the oxygen molecule may alter both electron spin and nuclear spin relaxation rates of cosolute spins through contact and dipole–dipole coupling mechanisms (*2*). The magnetic field dependence of spin–lattice relaxation rates, magnetic relaxation dispersion (MRD), provides an efficient method for characterizing both spin and molecular dynamics (*6, 7*). In paramagnetic systems, the MRD profile generally provides a direct report of the effective correlation times that dominate the electron-nuclear couplings. The correlation times may include contributions from translational diffusion, rotational diffusion, the electron spin relaxation times, and chemical exchange times when they are relevant as in a labile paramagnetic metal–ligand complex (*8, 9*). We have measured ^{1}H MRD profiles for several solvents in equilibrium with oxygen or air in order to understand what correlation time dominates the electron-nuclear couplings in oxygenated solutions. The essential result is that the effective correlation time for the intermolecular electron–proton coupling has contributions from both translational diffusion and the electron spin–lattice relaxation time, T_{1e}. However, T_{1e} is found to be approximately 7.5 ps and practically independent of solvent and viscosity.

EXPERIMENTAL

Cyclohexane (100%, CAS No: 110-82-7), benzene (100%, CAS No: 71-43-2), acetonitrile (99.9%, CAS No: 75-05-8), and dimethyl sulfoxide (99.9%, CAS No: 67-68-5) were purchased from J. T. Baker Inc. (Phillipsburg, NJ). Glycerol (99.8%, CAS No: 56-81-5), methanol (100%, CAS No: 67-56-1), and acetone (99.7%, CAS No: 67-64-1) were purchased from Mallinckrodt Baker Inc. (Paris, KY). Distilled and deionized water (resistance $>$ 17.5 MΩ) was drawn from a Barnstead NANOpure (Barnstead, Dubuque, IA) ultrapure water system that used house deionized water as the feed.

All solvents except for water–glycerol solution (50% by weight) were equilibrated with a continuous flow of oxygen (99.995%, BOC Gases, Murray Hill, NJ) for at least 8 h before measurements were taken. The glycerol sample was prepared in equilibrium with air to eliminate microbubble formation in the highly viscous solution. Samples were sealed in threaded Delrin or polycarbonate sample holders with nylon screws that compressed silicone O-ring cord-stock plugs (*10*). All surfaces in contact with the samples were washed with 0.1 M EDTA solution and dried in an oven prior to use.

The magnetic relaxation dispersion data were obtained using a dual magnet spectrometer described elsewhere (*10*). This spectrometer employs a modified Magnex superconducting 7.05 T solenoid operating in close proximity to a GMW 4-inch variable field electromagnet, which is magnetically isolated by an iron shield. The nuclear spin system is polarized in the high-field magnet, shuttled pneumatically to the remote electromagnet where the magnetization evolves for a variable time. The sample is then pneumatically returned to the high-field environment where the remaining magnetization is promptly detected. The experiments were performed at ambient laboratory temperature, maintained at approximately 294 K. Nonlinear fits to the data were performed using the Igor 3.21 (WaveMatrix, Inc., Lake Oswego, OR) for the MacIntosh computer

1090-7807/01 $35.00

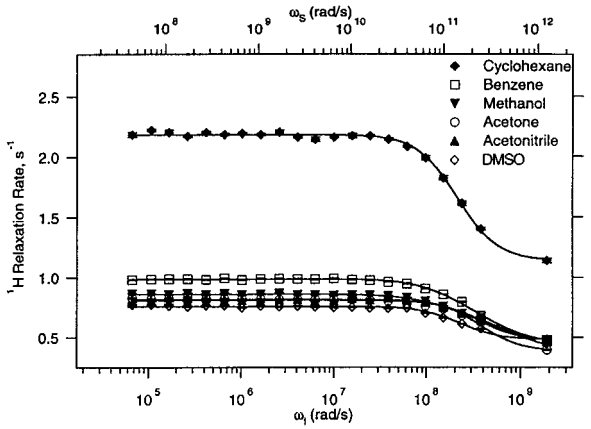

FIG. 1. Proton spin–lattice relaxation rates measured as a function of the magnetic field strength reported as the proton Larmor frequency (bottom) and electron Larmor frequency (top) for cyclohexane (◆), benzene (□), methanol (▼), acetone (○), acetonitrile (▲), and dimethyl sulfoxide (◇) at laboratory temperature. All samples were prepared in equilibrium with 1 atm of oxygen.

platform and Mathematica 3.0 (Wolfram Research Inc., Champaign, IL) for the Unix computer platform.

RESULTS AND DISCUSSION

Proton spin–lattice relaxation rates for cyclohexane, benzene, methanol, acetone, acetonitrile, and dimethyl sulfoxide equilibrated with oxygen at 1 atm are shown in Fig. 1 as a function of magnetic field strength plotted as the proton Larmor frequency on the bottom axis. The electron Larmor frequency is shown on the top axis. Data for aqueous systems are shown in Fig. 2 where the water was in equilibrium with 1 atm oxygen but the 50% glycerol solution was in equilibrium with air. In the absence of oxygen, there is no significant magnetic field dependence of the solvent–proton spin–lattice relaxation rate constants over the range of fields studied. The rotational and translational motions that dominate the proton–proton dipole–dipole contributions to nuclear spin relaxation disperse at Larmor frequencies more than an order of magnitude larger than those studied here because the correlation times are in the range of tens to hundreds of picoseconds. The internal chair–chair conformational interconversions in cyclohexane, which may be detected by spin–lattice relaxation dispersion measurements in the radiofrequency field (*11*), make no significant contribution to the dispersion in the Zeeman field because the relaxation contribution is proportional to the square of the chemical shift difference and, therefore, to the square of the magnetic field strength. The chair–chair interconversion would correspond to a dispersion near 1 MHz but at this low field the chemical shift differences are so small that the relaxation contribution is negligible compared with those from other relaxation mechanisms. Therefore, the magnetic relaxation dispersion observed in the proton relaxation rate of the different solvents in contact with oxygen derives from the paramagnetism of the dissolved oxygen.

The MRD profiles for the different solvents are remarkably similar. Different relaxation rates are expected because the relaxation rate is generally linear in the concentration of the paramagnetic center. However, the effective correlation time or the inflection frequency should not depend on the oxygen concentration unless the concentration becomes sufficiently large that oxygen–oxygen interactions become important. There is no evidence for oxygen–oxygen effects in these data.

The paramagnetic contribution to the relaxation dispersion profile is expected to be dominated by the relative translational motion of the oxygen molecule and the solvent protons. The relaxation equations for this problem have been developed by Freed and colleagues (*12*, *13*) and by Ayant *et al.* (*14*). These theories, which are appropriate for the current data set, include four parameters: the translational correlation time or the relative diffusion constant, the distance of closest approach between the interacting spins, the low-field electron spin relaxation time, and the correlation time for the electron spin relaxation process. The inflection frequencies in the data of Fig. 1 correspond to correlation times that are shorter than most measures of solvent–molecule translational correlation times. Thus, the electron relaxation time must make a significant contribution to the effective correlation time for the electron-nuclear coupling. The problem in fitting data to the translational relaxation equations is that the short electron spin relaxation time makes the fit relatively insensitive to the choices of the translational correlation time or, equivalently, the translational diffusion constant and the distance of closest approach. We minimize these problems by assuming the Lorentzian function in Eq. [1], which is the form of the translational model in the limit that the electron spin relaxation time is very short.

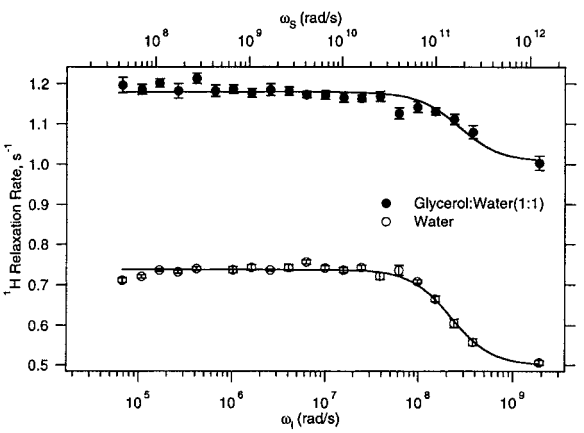

FIG. 2. Proton spin–lattice relaxation rates measured as a function of the magnetic field strength reported as the proton Larmor frequency (bottom) and electron Larmor frequency (top) for water (○) prepared in equilibrium with 1 atm oxygen and for 50% glycerol by weight prepared in equilibrium with 1 atm air (●).

TABLE 1
Electron Spin Relaxation Parameters

	τ (ps)	A ($\times 10^{10}$)	B
Cyclohexane	7.2 ± 0.2	4.9 ± 0.2	1.14 ± 0.02
Benzene	5.2 ± 0.2	3.3 ± 0.2	0.47 ± 0.01
Methanol (CH_3)	4.5 ± 0.3	3.1 ± 0.3	0.43 ± 0.02
Acetone	4.0 ± 0.2	3.6 ± 0.3	0.38 ± 0.02
Acetonitrile	4.2 ± 0.3	2.7 ± 0.2	0.47 ± 0.01
DMSO	6.7 ± 0.4	1.4 ± 0.1	0.48 ± 0.01
Glycerol/water (1:1)	5.7 ± 0.9	3.0 ± 0.7	1.00 ± 0.01
Water	6.8 ± 0.5	1.2 ± 0.1	0.50 ± 0.01

$$\frac{1}{T_1} = A\left[\frac{\tau}{1 + \omega_S^2\tau^2}\right] + B, \qquad [1]$$

where A and B are constants, ω_S is the electron Larmor frequency, and τ is the correlation for the electron-nuclear coupling. This equation is based on the more general form,

$$\frac{1}{T_1} = A[3J(\omega_I) + 7J(\omega_S)], \qquad [2]$$

where $J(\omega_{I,S})$ are spectral densities at the nuclear and electron Larmor frequencies, respectively (*15–17*). Thus, the first term in Eq. [1] includes the dispersion from the electron Larmor frequency and the constant, B, includes the contribution associated with the nuclear Larmor frequency or the $J(\omega_I)$ term as well as the field-independent diamagnetic contribution. The factor A is a function of the magnetogyric ratios of the proton and the electron, the dissolved oxygen concentration, the intermoment distance, and the usual physical constants. We note that the Delrin sample shuttle used in these experiments is not completely impervious to oxygen. There may be a slight drift in the oxygen concentration during these experiments, which will appear as a variation in parameter A, but will not affect the conclusions. Polycarbonate sample holders leak oxygen quite rapidly. The results are summarized in Table 1 in terms of the parameters of Eq. [1] and are shown as the solid lines in Figs. 1 and 2. The entries in Table 1 show that the inflection frequency is only a weak function of the solvent choice despite the fact that the translational diffusion constants or viscosities for these solvents differ.

Figure 2 summarizes measurements made on water protons in water and in aqueous glycerol, 50% by weight, in equilibrium with air. The glycerol solution has a viscosity five times that of water, which will increase the correlation times for the translational and rotational motions that dominate proton–proton dipole–dipole couplings. Thus, the relaxation dispersion curve is shifted to higher relaxation rates. However, the inflection frequency is unchanged from that in water. Therefore, the translational and rotational motions make no effective contribution to the correlation time for the electron-nuclear coupling in the water–glycerol solutions. Figure 2 also shows that the amplitude of the relaxation dispersion or the difference between the high- and low-field relaxation rates is reduced significantly. This reduction is caused in part by the reduced oxygen partial pressure in air, which is partly compensated by increased oxygen solubility. A second factor is the probability that a water molecule is in contact with the paramagnetic relaxation center. In neat solvents, this factor is suppressed, but included as a scaling factor that accounts quite well for the observations in dilute electrolyte solutions when the force-free conditions are relaxed (*18*). In the water–glycerol solution, the presence of glycerol excludes a certain volume from simultaneous occupancy by water adjacent to the oxygen. Although a detailed calculation is beyond the scope of this discussion, in a 50% solution by weight, the reduction expected is of order $\frac{1}{2}$.

The magnitudes of the effective correlation times shown in Table 1 do not change very much over the range of solvents studied. However, they are not completely independent of solvent. If the inflection frequency represented simply $1/T_{1e}$, all solvents would yield the same dispersion curve and the oxygen T_1 would be approximately 5 ps. However, this correlation time is close enough to translational correlation times that the translational motions may contribute to the effective correlation time. We may reintroduce the translational motion if we assume that the effective correlation time for the electron-nuclear coupling may be written as

$$\frac{1}{\tau} = \frac{1}{T_{1e}} + \frac{1}{\tau_{tr}}, \qquad [3]$$

where the translational correlation time, τ_{tr}, may be related to the relative diffusion constant, D_{rel}. Because the solute mobility is limited in part by the motion of the solvent, we may approximate the relative diffusion constant for the solvent and the oxygen as twice that of the solvent. Thus, we may write

$$\frac{1}{\tau_{tr}} \approx \frac{6(2D_{solvent})}{l^2}. \qquad [4]$$

l^2 is the mean jump length for the diffusive process, usually approximated as the diameter of the molecule, which is proportional to the $\frac{2}{3}$ power of the molar volume or, equivalently, the (molecular mass/density)$^{2/3}$. We may than write

$$\frac{1}{\tau} = \left(\frac{1}{T_{1e}}\right) + CD_{solvent}\left(\frac{mw}{\rho}\right)^{-2/3}, \qquad [5]$$

where C is a constant, mw the molecular weight, ρ the density, and $D_{solvent}$ the self-diffusion constant for the solvent, respectively. If the electron relaxation time is constant, then Eq. [5] is linear. The data of Table 1 are plotted according to Eq. [5] in Fig. 3, which shows that the effective correlation time for the electron-nuclear coupling in the nonaqueous solvents is rea-

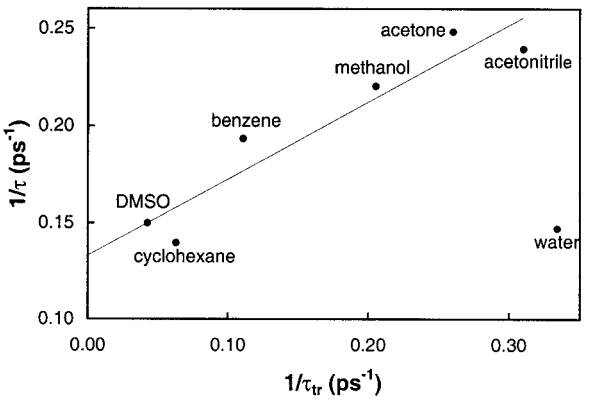

FIG. 3. The effective correlation rate plotted as the reciprocal of the effective correlation time, τ, plotted against $\{D_{\text{solvent}} \times (\text{molar volume})^{-2/3}\}$ as indicated in Eq. [5]. The solid linear regression line was calculated excluding the aqueous solution points and has an intercept of 0.13, corresponding to an oxygen T_{1e} of 7.5 ps in solution.

sonably well represented by this simple model. The intercept corresponds to an average electron spin–lattice relaxation time of 7.5 ps.

Water is an exception. Further, the inflection point for 50% glycerol solution corresponds to an electron relaxation time of 5.7 ± 0.7 ps, which is within the experimental error of that for water. The major difference between water and the other solvents is the increased opportunity for strong hydrogen bonds with the oxygen, which apparently decouples the effective electron-nuclear correlation time from the translational dynamics of the solvent. Estimates for hydrogen bond lifetimes are difficult, but are generally shorter than times of order 10 ps. Thus, the uncoupling of translational motions from the effective correlation time for proton–oxygen coupling may be a cooperative process involving water–water interactions that slow the apparent motions of the protons near the oxygen molecule (*19*).

It is important to note that, while this discussion is self-consistent, the differences in the effective correlation times are small and not far outside the errors. However, these experiments demonstrate that the oxygen electron T_1 is short, between 5 and 10 ps. Similar results for oxygen spin–lattice relaxation times have been reported based on measurements in fluorocarbons (*20–23*). The insensitivity of the oxygen spin–lattice relaxation time to the local environment of the oxygen molecule suggests that the electron relaxation mechanism is not strongly coupled to the oxygen molecule motions such as rotational tumbling or translation. This result greatly simplifies the interpretation of experiments in which the oxygen paramagnetism is used to probe interactions with cosolute macromolecules by measuring the oxygen-induced changes in macromolecule ^{1}H spin–lattice relaxation rates.

ACKNOWLEDGMENTS

This work was supported by the National Institutes of Health, GM34541 and GM54067. We appreciate helpful discussions with Jack Freed and the assistance of Charles Holmes and Shawn Wagner.

REFERENCES

1. C.-L. Teng and R. G. Bryant, *J. Am. Chem. Soc.* **122,** 2667–2668 (2000).
2. R. Hausser and F. Noack, *Z. Naturforsch.* **20A,** 1668–1675 (1965).
3. W. Froncisz, C. S. Lai, and J. S. Hyde, *Proc. Natl. Acad. Sci. USA* **82,** 411–415 (1985).
4. W. K. Subczynski and J. S. Hyde, *Biophys. J.* **45,** 743–748 (1984).
5. W. K. Subczynski and J. S. Hyde, *Biochem. Biophys. Acta* **643,** 283–291 (1981).
6. F. Noack, NMR field cycling spectroscopy: Principles and applications. *Progr. NMR Spectrosc.* **18,** 171–276 (1986).
7. S. H. Koenig and R. D. Brown III, *Prog. Nucl. Magn. Reson. Spectrosc.* **22,** 487–567 (1991).
8. I. Bertini and C. Luchinat, "NMR of Paramagnetic Molecules in Biological Systems," Benjamin/Cummings, Menlo Park, CA, 1986.
9. L. Banci, I. Bertini, and C. Luchinat, "Nuclear and Electron Relaxation," VCH, Weinheim, 1991.
10. S. Wagner, T. R. J. Dinesen, T. Rayner, and R. G. Bryant, *J. Magn. Reson.* **140,** 172–178 (1999).
11. H. Deveaux, N. Birlirakis, C. Wary, and P. Berthault, *Mol. Phys.* **86,** 1059–1073 (1995).
12. L. P. Hwang and J. H. Freed, *J. Chem. Phys.* **63,** 4017 (1975).
13. J. H. Freed, *J. Chem. Phys.* **68,** 4032 (1978).
14. Y. Ayant, E. Belorizky, J. Alizon, and J. Gallice, *J. Phys.* **36,** 991 (1975).
15. I. Solomon, *Phys. Rev.* **99,** 559 (1955).
16. I. Solomon and N. Bloembergen, *J. Chem. Phys.* **25,** 261 (1956).
17. N. Bloembergen and L. O. Morgan, *J. Chem. Phys.* **34,** 842 (1960).
18. T. R. J. Dinesen, J. Seymour, L. McGowan, S. Wagner, and R. G. Bryant, *J. Phys. Chem.* **103,** 782–786 (1999).
19. D. W. Davidson, in "Water: A Comprehensive Treatise," (F. Franks, Ed.), pp. 115–234, Plenum Press, New York, 1973.
20. J. J. Delpuech, M. A. Hamza, G. Serratrice, and M.-J. Stebe, *J. Chem. Phys.* **70,** 2680–2687 (1979).
21. M. A. Hamza, G. Serratrice, M.-J. Stebe, and J.-J. Delpuech, *J. Am. Chem. Soc.* **103,** 3733–3738 (1981).
22. M. A. Hamza, G. Serratrice, M.-J. Stebe, and J.-J. Delpuech, *J. Magn. Reson.* **42,** 227–241 (1981).
23. M.-J. Stebe, G. Serratrice, and J.-J. Delpuech, *J. Phys. Chem.* **89,** 2837–2843 (1985).